of protons, and perhaps the parameters in the level-density formula need to be specially adjusted for this situation. It would seem that much more experimental evidence needs to be obtained to discover systematics which may exist.

CONCLUSION

The results of the present experiment suggest that the statistical theory of nuclear reactions describes adequately, at least, the shapes of the energy spectra of light particles from nitrogen-induced reactions at zero degrees. Angular distributions and experiments on heavier targets have yet to be explored. Heavy-ion reactions might provide a useful means of measuring statistical aspects of nuclear structure.

ACKNOWLEDGMENTS

The authors gratefully acknowledge their indebtedness to John G. Harris for constructing the proportional counters and mechanical apparatus, to Gertrude Foster for carrying out the cross-section calculations and for constructing graphs used in the analysis of the data, to A. Zucker for help and encouragement, and to R. S. Livingston for interest in and support of the experiment.

PHYSICAL REVIEW VOLUME 110, NUMBER 3 MAY 1, 1958

Elastic and Inelastic Scattering of 18-Mev Alpha Particles from Neon, Argon, and Xenon*

L. SEIDLITZ,† E. BLEULER, AND D. J. TENDAM
Department of Physics, Purdue University, Lafayette, Indiana
(Received November 5, 1957)

The scattering of 18-Mev alpha particles from neon, argon, and xenon was studied with a multiplate reaction chamber. The scattered particles were defined within an rms angular width of 0.45° by a system of slit pairs, spaced every 2½° from 10° to 170°. The elastic scattering from neon and argon show the pronounced maxima and minima characteristic of diffraction scattering but are equidistant in ϕ, not $\sin(\phi/2)$. The ratio to Rutherford scattering varies as much as 25-fold between successive maxima and minima in the case of neon, the well-defined structure indicating a small mean free path for absorption of alpha particles in the nucleus. Nuclear interaction radii calculated by the formula $2kR\Delta[\sin(\phi/2)]=\pi$ were found to be 6.36×10^{-13} cm for neon and 6.95×10^{-13} cm for argon. Xenon, investigated chiefly for control purposes, showed no definite deviation from Rutherford scattering up to 50°. Groups corresponding to the excitation of the 1.63-, 4.25-, 4.97-, 5.81(5.63)-, and 7.2-Mev levels of Ne^{20} and the 1.46-Mev level of A^{40} were observed. No excited states were observed in xenon. Notably absent was excitation of the 6.74-Mev (0^+) level in Ne^{20}. As predicted by direct-interaction theories, the cross sections for inelastic scattering leading to the first excited (2^+) states of neon and argon could be approximated by the squares of spherical Bessel functions of the second order with interaction radii of 6.71×10^{-13} cm for neon and 6.60×10^{-13} cm for argon. These cross sections do not tend toward small values in the forward direction, which is interpreted as evidence for distortion of the incident and scattered waves. No fit was possible for any of the other excited states.

INTRODUCTION

THERE has been renewed interest in the scattering of alpha particles from nuclei following the establishment by Farwell and Wegner[1] of a pronounced variation with energy of the scattering cross section for heavy nuclei. They found that the ratio of the observed differential scattering cross section to the Rutherford cross section, $\sigma(E)/\sigma_R(E)$, was unity only for energies below certain values and decreased exponentially with higher energies. Further experiments on alpha-particle scattering from heavy nuclei were performed by Wall, Rees, and Ford,[2] Wegner, Eisberg, and Igo,[3] Ellis and Schecter,[4] and Gove,[5] all of whom measured the angular dependence of the cross sections. When the cross sections are plotted as functions of the apsidal distance of the classical path in a pure Coulomb field, the results are similar to those found by Farwell and Wegner: agreeing with the Rutherford cross section for the large apsidal distances, followed by an exponential fall-off toward the smaller.

Since these results were in striking contrast to the diffraction-like angular distributions found in the scattering of protons from various nuclei,[6] Bleuler and Tendam[7] and Eisberg, Igo, and Wegner[8] investigated the scattering of alpha particles from light nuclei. They found the expected diffraction patterns at bombarding energies of 19 Mev with aluminum and copper and of 40 Mev with aluminum, respectively. Subsequent to the start of the investigation reported here, more extensive measurements on light nuclei were published by Igo, Wegner, and Eisberg[9] at 40 Mev, by Gugelot

* Work supported in part by the U. S. Atomic Energy Commission. This article is based on a doctoral thesis submitted by L. Seidlitz to the Faculty of Purdue University. A short report was given in Bull. Am. Phys. Soc. Ser. II, 1, 29 (1956).
† Now at Palmer Physical Laboratory, Princeton University, Princeton, New Jersey.
[1] G. W. Farwell and H. E. Wegner, Phys. Rev. **95**, 1212 (1954).
[2] Wall, Rees, and Ford, Phys. Rev. **97**, 726 (1955).
[3] Wegner, Eisberg, and Igo, Phys. Rev. **99**, 825 (1955).
[4] R. E. Ellis and L. Schecter, Phys. Rev. **101**, 636 (1956).
[5] H. E. Gove, Phys. Rev. **99**, 1353 (1955).
[6] B. L. Cohen and R. V. Neidigh, Phys. Rev. **93**, 282 (1954).
[7] E. Bleuler and D. J. Tendam, Phys. Rev. **99**, 1605 (1955).
[8] Eisberg, Igo, and Wegner, Phys. Rev. **99**, 1606 (1955).
[9] Igo, Wegner, and Eisberg, Phys. Rev. **101**, 1508 (1956).

and Rickey[10] at 42 Mev, and by Watters[11] at 32 Mev, in which the angular distributions also showed maxima and minima.

The interpretation of the measurements is made tedious by the large number of partial waves involved, as evidenced by the large number of maxima and minima. Though semiclassical models have had good success in explaining the scattering from heavy nuclei,[2,4,12,13] the best results are to be expected from an analysis by means of the optical model.[14–16] This model has had success in fitting the angular distributions found in neutron[16,17] and proton[18,19] scattering. Recently, excellent theoretical agreement has been obtained for alpha-particle scattering.[20,21] It is hoped that eventually the optical-model parameters for the alpha-nucleus system will be obtained for various energies.

Without an optical-model analysis, the only parameter that may be determined from the angular distribution obtained with a light nucleus is an interaction radius. It may be calculated, according to the Born-approximation formula for the scattering from a square well, by identifying the minima with the zeros of $j_1(qR)=j_1[2kR\sin(\phi/2)]$,[10] or more simply, and probably with equal justification, by putting the difference of the qR values for neighboring minima (or maxima) equal to $\Delta(qR)=2kR\Delta[\sin(\phi/2)]=\pi$. Here, j_1 is the spherical Bessel function of order one, q the magnitude of the difference between the initial and final wave vectors, R an "interaction radius," k the wave number of the system, and ϕ the scattering angle in the center-of-mass system. By application of this relation to those cases where the spacings are fairly equidistant, reasonable values for the interaction radii have been deduced.[7,9]

For the light elements, the elastically scattered alpha particles are always accompanied by alpha groups due to inelastic scattering. The differential cross section is found to vary strongly with angle, suggesting a reaction mechanism other than compound-nucleus formation. Direct interactions between an incoming nucleon and either a surface nucleon or the nuclear surface (the former leading to inelastic or exchange scattering, the latter to a collective, rotational excitation) have been considered by Austern, Butler, and McManus[22] and by Hayakawa and Yoshida,[23] respectively. The angular

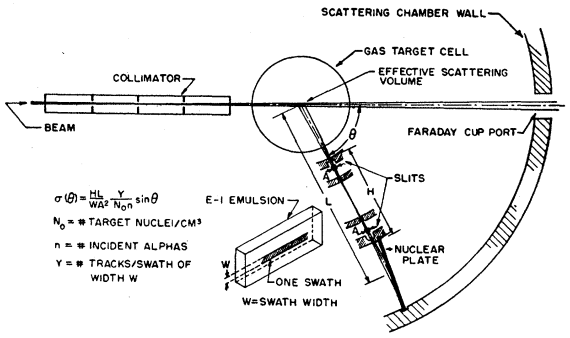

FIG. 1. Scattering chamber geometry.

distributions as calculated by Austern *et al.* in the plane-wave approximation are given by expressions of the form $\sum a_l[j_l(qR)]^2$. For the excitation of the first rotational level in particular, Hayakawa and Yoshida determine the angular factor to be $[j_2(qR)]^2$. The analysis of Austern *et al.* may, in main outline, be applicable to inelastic scattering of alpha particles.[24] Several experimenters[10,11,25] have had fair success in fitting distributions of inelastically scattered alpha particles with spherical Bessel functions. The inadequacy of these analyses lies chiefly in the assumption of incident and scattered plane waves. The existence of strong potential wells (~30–40 Mev) for the alpha-particle-nucleus interaction as required by optical-model analyses[20,21] results in distortion of both incident and scattered waves. Levinson *et al.*[26] have shown in the case of inelastic proton scattering that good agreement between theory and experiment may be achieved if the distortion of the incident and scattered waves produced by the Coulomb and nuclear fields is taken into account.

The investigations herein reported are a continuation of the preliminary work of Bleuler and Tendam.[7] Because rapidly varying intensities were expected, the measurements were made at $2\frac{1}{2}°$ intervals with improved angular resolution. To investigate such aspects as the possibility of symmetry about 90° and the effect of distortion in the forward direction, the angular range was extended to limits of 10°–170°. Nuclear emulsions were chosen as detectors to supplement concurrent investigations[27] being done with electronic techniques. In these latter investigations, thin foils were used as targets. Because of this fact and the availability of an extremely thin-walled gas cell of large angular aperture, nuclides not obtainable as thin foils were chosen as targets. These were neon, argon, and xenon; neon being representative of a light nucleus and argon a medium-weight nucleus. Xenon was included since it was

[10] P. C. Gugelot and M. Rickey, Phys. Rev. **101**, 1613 (1956).
[11] H. J. Watters, Phys. Rev. **103**, 1763 (1956).
[12] J. S. Blair, Phys. Rev. **95**, 1218 (1954).
[13] C. E. Porter, Phys. Rev. **99**, 1400 (1955).
[14] H. A. Bethe, Phys. Rev. **57**, 1125 (1940).
[15] Fernbach, Serber, and Taylor, Phys. Rev. **75**, 1352 (1949).
[16] Feshbach, Porter, and Weisskopf, Phys. Rev. **96**, 448 (1954).
[17] Culler, Fernbach, and Sherman, Phys. Rev. **101**, 1047 (1956).
[18] Glassgold, Cheston, Stein, Schuldt, and Erickson, Phys. Rev. **106**, 1207 (1957).
[19] Melkanoff, Nodvik, Saxon, and Woods, Phys. Rev. **106**, 793 (1957).
[20] W. B. Cheston and A. E. Glassgold, Phys. Rev. **106**, 1215 (1957).
[21] G. Igo and R. M. Thaler, Phys. Rev. **106**, 126 (1957).
[22] Austern, Butler, and McManus, Phys. Rev. **92**, 350 (1953).
[23] S. Hayakawa and S. Yoshida, Proc. Phys. Soc. (London) **A68**, 656 (1955); and Progr. Theoret. Phys. (Japan) **14**, 1 (1955).
[24] S. T. Butler, Phys. Rev. **106**, 272 (1957).
[25] F. J. Vaughn, University of California Radiation Laboratory Report UCRL-3174, October, 1955 (unpublished).
[26] Levinson, Banerjee, Albright, and Tobocman, Bull. Am. Phys. Soc. Ser. II, **1**, 194 (1956); C. A. Levinson and M. K. Banerjee, Ann. Phys. **3**, 67 (1958).
[27] O. Gailar, Ph.D. thesis, Purdue University, August, 1956 (unpublished).

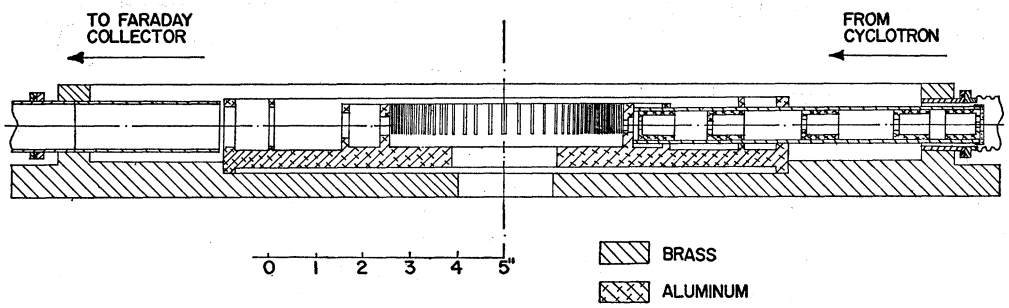

FIG. 2. Cross section of the scattering chamber.

expected that at the bombarding energy used (18 Mev) its nuclear charge was large enough to produce Rutherford scattering. Furthermore, neon and argon each have a well-known, isolated first excited state to provide a comparison of the inelastic scattering with direct-interaction theories.

EXPERIMENTAL METHOD AND EQUIPMENT

Scattering Chamber

The 19-Mev alpha-particle beam from the Purdue cyclotron, focused by a magnetic quadrupole lens, was brought through the water tank shielding, collimated, and made to impinge on a gas target in the center of a scattering chamber. The reaction products, defined in angle by a system of slit pairs, were detected by a number of nuclear track emulsions, one of which was located behind each pair of slits. The undeflected beam was collected in a Faraday cup, the total charge collected being integrated electronically.

The scattering chamber is shown in Figs. 1 and 2. The chamber proper is a cylindrical brass box of 18 in. inside diameter and $1\frac{3}{4}$ in. internal depth with a removable aluminum lid. The base of the chamber is recessed and provided with a pin to align the analyzing slit system precisely. By means of selective shutters, the entire range of available angles can be exposed with one loading of the chamber despite the enormous variation in intensity (e.g., $\sim 10^7$ for argon).

The collimator is a brass tube containing six concentric circular diaphragms. The first diaphragm, which intercepts most of the nontransmitted beam, is machined from bismuth, thus reducing the neutron and gamma-ray background. It is immediately in front of, and only slightly larger in aperture than the first of the two actual collimating diaphragms which are $\frac{1}{16}$ in. in diameter. The latter two restrict the transmitted beam to a cone of 0.5° half-angle. The remaining three diaphragms are slightly larger than the collimating diaphragms and are located between them. They are so positioned that a beam particle scattered from the collimating tube wall cannot emerge without an additional scatter. This effectively makes the collimator wall-less. All diaphragms but the first are aluminum. The collimator is held in the analyzing slit system, the inner ring of which serves as a forward stop. The distance of the collimator from the target is such that the beam diameter at the center of the chamber can be no greater than 0.10 in., if one ignores multiple scattering in the target cell. It was found necessary to surround the front end of the collimator with a lead shield to avoid heavy gamma-ray and neutron background in the plates nearest the collimator.

The target cell is of novel construction. Its wall is a film of Mylar, 0.0005 in. thick, which is supported by narrow struts so that scattered particles are essentially unobstructed in the angular range 10° to 170°. The Mylar film is cemented to the brass frame with Armstrong Adhesive A-1.[28] A hole drilled through the cell base allows the target cell to be evacuated and filled with the target gas. The gas-handling system screws onto the base and is suspended therefrom. A mercury manometer indicates the gas pressure and was read with a cathetometer to the nearest 0.1 mm. The pressures used were 20 cm for neon and argon and 5 cm for xenon.

The analyzing slit system consists of an inner and an outer ring of slits which define the directions of detected particles and two central rings of slits which assure their radial passage. The entire system is integrally constructed, having been machined from a single casting. The outside diameter is 12 in.; the slit width is $\frac{1}{16}$ in. and the acceptance width is $\pm 1°$ from the nominal scattering angle. Slits are spaced every five degrees, but are machined on both sides of the beam direction in such a manner that measurements can be made every $2\frac{1}{2}°$ in the interval 10°–170°. A pair of slits is provided at $\pm 20°$ as an aid for correction of possible chamber misalignment after the bombardment is completed.

The chamber was mounted on a rolling cart and was evacuated by its own vacuum system prior to connecting it to the cyclotron. The cart also carried mechanisms for remotely adjusting the chamber axis with respect to the beam direction. A beam-range measuring device[29,30] was mounted at the end of the beam pipe,

[28] Available from Armstrong Adhesive Company, Warsaw, Indiana. More recently Dupont Polyester Adhesive has been utilized. For further details of the construction of the cell see Corelli, Livingston, and Seidlitz, Rev. Sci. Instr. 28, 471 (1957).

[29] R. L. Clary, M.S. thesis, Purdue University, 1950 (unpublished).

[30] Gailar, Seidlitz, Bleuler, and Tendam, Rev. Sci. Instr. 24, 126 (1953).

directly in front of the chamber. The energy was determined by use of the range-energy relation for alpha particles in aluminum derived from the curves given by Bethe.[29,31]

Photographic Technique

Ilford $E1$ nuclear track emulsions, 50 or 100 microns thick, 1 in.×3 in., were used. To make reasonable the rate of acquisition of data and to make possible the use of previously untrained observers, it was necessary to develop a method of discriminating reliably between tracks due to alpha particles and those due to protons or deuterons, by a rapid inspection without resort to quantitative measurements. This goal was accomplished by the use of latent-image fading and differential development. Both latent-image fading and differential development (through the use of a strongly proportional inhibitor combined with underdevelopment) enhance the relative development of those grains most highly activated, i.e., those traversed by an alpha particle.

The developer used was substantially that due to Billington[32] but the developing times were somewhat altered. An example of the result is found in Fig. 3. There are apparent two kinds of tracks, referred to for convenience as "light" and "dark." With a little experience, virtually all tracks longer than 10 microns can be classified at a glance as being one or the other. To confirm that this rapidly made, qualitative classification corresponded to distinguishing between tracks made by protons (and deuterons) or by alpha particles respectively, grain-density measurements were made upon a number of tracks.

The plate used for this measurement had been exposed in another experiment; 10-Mev deuteron bombardment of Teflon, $(C_2F_4)_m$. The bulk of the tracks were due to elastically scattered deuterons (~300-micron range). Some of the tracks due to protons could be identified simply because they were longer than those due to the most energetic deuteron or alpha particle (~85-micron range). The procedure used was as follows:

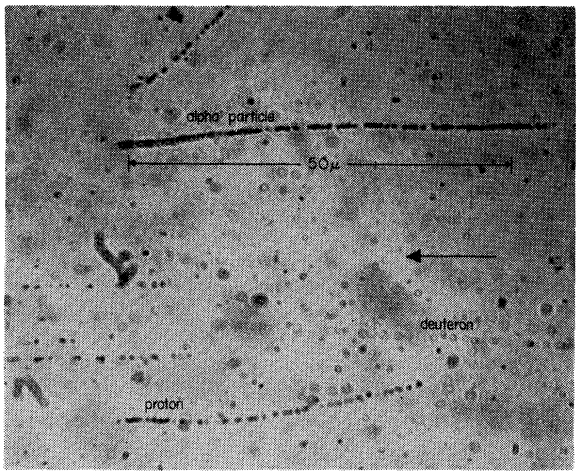

FIG. 3. Differentially developed tracks in $E1$ emulsion.

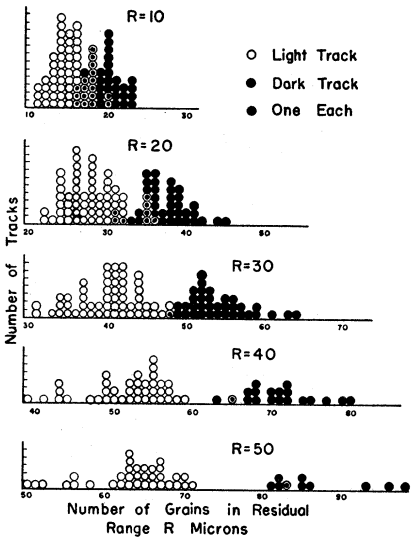

FIG. 4. Grain density histograms.

Each track as it came onto the eyepiece measuring scale was recorded as L or D (light or dark), its length was measured, and the number of grains per ten-micron interval for 5 intervals from the *end* of the track was counted. Only a few long tracks which were known to have been made by deuterons or protons were measured. Histograms were then made showing the frequency of total number of grains for various residual ranges (see Fig. 4). For residual ranges of 30 microns or more, the L and D tracks fall into two distinct groups with very few exceptions. The two groups are statistically resolvable in the case of 20-micron range, but the grain density is definitely unreliable as a means of discrimination for 10-micron residual range. Criteria which are more subjective can be used to give confidence in the choice of L or D for the tracks which fell into the "wrong" group. The greater scattering of protons (and deuterons) for a given range generally aids in the identification but more reliably the effect of the partial development is to give an appearance of "thinness" to the proton tracks which is not reflected in the grain density measurement. In fact, the smaller grains of the proton tracks make it less probable that two or more grains will overlap and be counted as one grain, as frequently will happen for alpha-particle tracks. This results in a loss of resolution in the grain-density histograms but actually aids the visual distinction between L and D. It is the latter effect which allows reliable, subjective distinction down to tracks as short

[31] Hans A. Bethe, Brookhaven National Laboratory Report BNL-T-7, 1949 (unpublished).

[32] Roberts, Solano, Wood, and Billington, Rev. Sci. Instr. 24, 920 (1953).

as 10 microns where the objective grain density measurement fails.

Acceptance criteria were established to prevent the recording of spurious tracks and to control the area that was scanned. Added confidence in the method of discrimination was gained by the fact that there were virtually no dark, spurious tracks, i.e., tracks that did not enter the surface of the emulsion in the proper direction.

The sole measurement made on most accepted tracks was that of projected length. If a track (otherwise satisfactory) left the emulsion, a notation was entered. This was done to check the possibility that a significant number of tracks might leave the emulsion and thereby distort the range distribution. There were very few such tracks, about $\frac{1}{2}\%$ of the total. For less than 1% of the tracks counted, dip and scatter had also to be accurately measured so that the rectified length could be computed. It is apparent that the complication of the mechanical construction of the slit system was justified by the ease of rejection of spurious tracks and by the single datum required of most tracks.

REDUCTION OF DATA AND SOURCES OF ERROR

The data were corrected for second-order geometrical effects by using the analysis of Critchfield and Dodder[33] properly modified for the present arrangement. The rms deviation in angle due to the finite geometry is 0.45° and that due to multiple scattering in the Mylar window and the target gas is 0.63° in the most unfavorable cases. The largest corrections were 8% for neon at 15° and 5.5% for argon at 12.5°. The corrections at these forward angles were equivalent to a correction of about 0.1° in the nominal scattering angle and were within the experimental uncertainty in the determination of the angle.

The uncertainties in the geometrical factors in the expression for the cross sections are negligible, being in most cases fractions of a percent. Also found negligible were errors due to target gas heating and to variation of the incident energy within the scattering volume. The latter conclusion was based upon the assumption that the cross section varied no more rapidly than inversely as the square of the energy.

The chief uncertainty in the final values of the cross sections is that due to the statistical reliability of the number of tracks measured. For the neon elastic cross section this is generally about 6% except that at some of the minima it is 10% (all errors are given as standard deviations). For the argon elastic cross section it is 6% wherever possible. At some angles the entire plate was scanned but this reliability could not always be achieved and in one case it is as poor as 33%. The detailed values are given in the next section together with the results.

The positions of the individual plates are accurate to better than $\pm 0.1°$ but since there was a larger uncertainty in the location of the zero angle, the angular uncertainties are: 10° to 20°, $\pm 0.18°$; 25° to $32\frac{1}{2}°$, $\pm 0.27°$; $\theta \geqslant 37\frac{1}{2}°$, $\pm 0.32°$.

Even these small errors in the forward angles lead to large uncertainties in the determination of $\sigma(\phi)/\sigma_R(\phi)$ due to the steepness of the Rutherford cross section in that region. These uncertainties are 9.0% at 10°, 7.2% at $12\frac{1}{2}°$, 5.7% at 15°, 4.3% at 20°, 5.1% at 25° and 4.2% at 30° and less than 4% at larger angles.

In the case of neon, there is an additional and somewhat disturbing uncertainty. The early-model target chamber used for neon did not allow the simultaneous exposure of all plates. Two runs were needed and, therefore, errors in current integration or the temperature and pressure of the gas result in relative uncertainties. The current integrator is reliable to about 2%, while the gas density measurement has still smaller uncertainty. In some regions the points from the two runs do not agree, the second run giving the larger cross sections, at some angles as much as 20% larger. A constant factor such as would arise, say, from a gross misreading of the current integrator, could not remedy matters since the discrepancy is not uniform. Furthermore, the minima and maxima of the two runs do not always agree, although it is difficult to be sure of this because the structure of the oscillations is fine compared to the spacing of angles in a single run. It may be that the positions of the minima are strongly energy-dependent. The average energies in the two runs were slightly different: 18.10 and 17.94 Mev, respectively. The cross-section curve was drawn giving equal weight to both runs.

The absolute accuracy of the energy determination was about 1%. The ranges in the plates compared well with those predicted from the calculated energy and Rotblat's range-energy curves in Ilford emulsion[34] after account was taken of the additional uncertainties introduced by allowing for loss of range due to passage through the Mylar wall and the target gas. The loss of range was calculated by the use of the relation of Heller and Tendam.[35] The energy enters into the results for $\sigma(\phi)/\sigma_R(\phi)$ as $1/E^2$, the uncertainty introduced in this ratio being then 2%.

EXPERIMENTAL RESULTS AND DISCUSSION

Nuclear Energy Levels

Typical range-number histograms of the alpha particles scattered from neon, argon, and xenon are shown in Fig. 5. Groups corresponding to elastic scattering and to excitation of the 1.63-, 4.25-, 4.97-, 5.81-,[36] and 7.2- (7.18 and 7.22 unresolved) Mev levels in Ne^{20} are

[33] C. L. Critchfield and D. C. Dodder, Phys. Rev. **75**, 419 (1949).

[34] J. Rotblat, Nature **167**, 550 (1951).

[35] Z. H. Heller and D. J. Tendam, Phys. Rev. **84**, 905 (1951).

[36] More recently, the energy of this level has been given as 5.63 Mev [W. W. Buechner and A. Sperduto, Phys. Rev. **106**, 1008 (1957)].

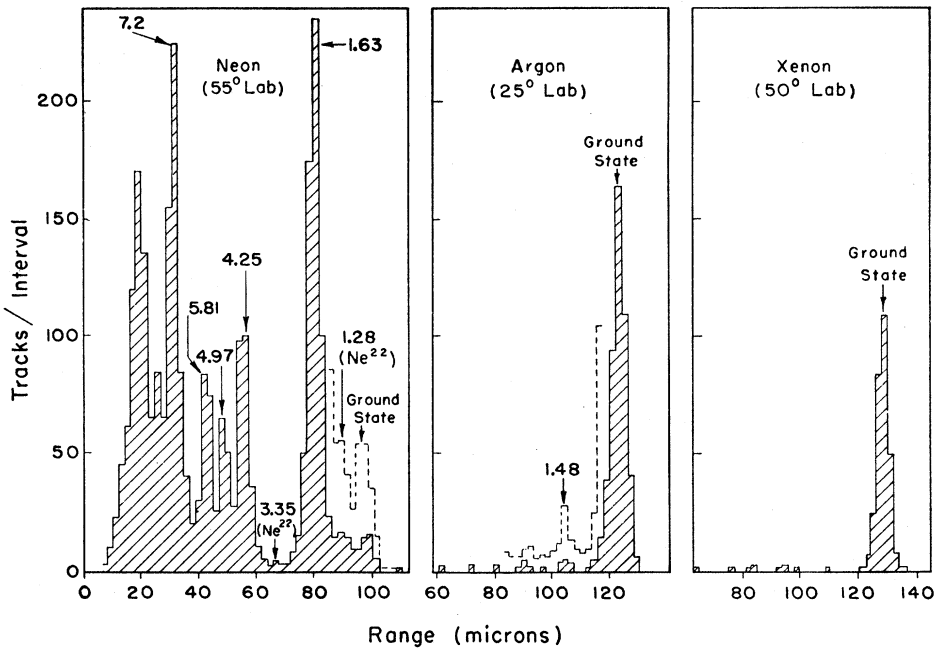

FIG. 5. Range distributions of alpha particles scattered from Ne, A, and Xe.

shown. The first four energy values, taken from Sperduto and Buechner,[37] agree well with the location of the peaks whereas the energies given in the compilation of Ajzenberg and Lauritsen[38] would be incompatible. The upper limit for excitation of the 6.74-Mev level[38] (not observed here) is about 1 millibarn/steradian. Groups from levels of higher excitation were observed but not resolved, nor was the elastic scattering from Ne^{22} (isotopic abundance 8.8%) resolved. Groups resulting from excitation of the 1.28- and 3.35-Mev levels in Ne^{22} were observed at some angles but not in sufficient intensity to determine an angular distribution. At most angles the only distinct groups found in the scattering from argon were those due to elastic scattering and to excitation of the 1.46-Mev first excited state of A^{40}. Elastic scattering only was observed from xenon.

Elastic and Inelastic Scattering Differential Cross Sections

The values for various differential cross sections for neon and argon are listed in Table I. (All cross sections are in the center-of-mass system.) The differential cross sections, $\sigma_0(\phi)$ and $\sigma_1(\phi)$, for the scattering from the ground and first excited states, respectively, of Ne^{20} are plotted in Fig. 6 together with $\sigma_R(\phi)$. In Fig. 7, the ratio $\sigma_0(\phi)/\sigma_R(\phi)$ is shown. There is structure in σ_0 in the very forward direction, σ_0/σ_R having a maximum at 14°. The spacing of maxima is approximately equidistant in ϕ, not $\sin(\phi/2)$, in contradistinction to the conclusions of some other observers[7,9,11] whose range of angles did not extend so far backward. It is interesting to note that the first three oscillations of the two cross sections are "out-of-phase" but that the remainder are "in-phase." The magnitudes of the cross sections are about equal for $\phi > 70°$. The positions of the first four minima of σ_0/σ_R were inserted in the relation R

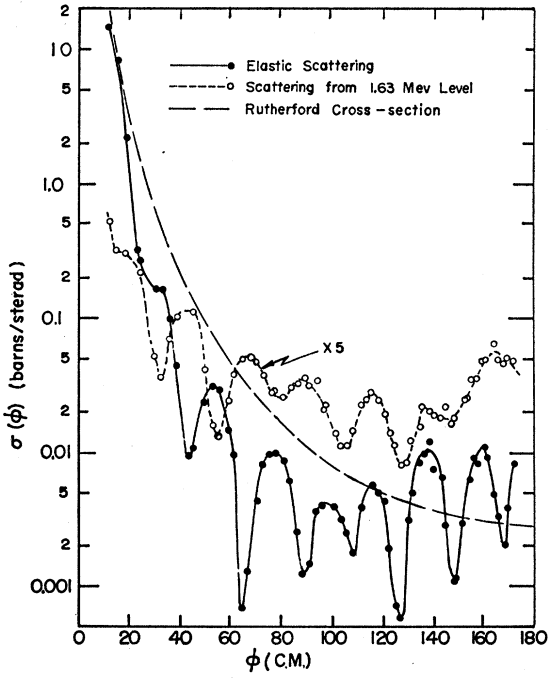

FIG. 6. Scattering cross sections for Ne. $E_\alpha = 18.0$ Mev.

[37] A. Sperduto and W. W. Buechner, Massachusetts Institute of Technology Annual Progress Report No. 38, May 31, 1955 (unpublished).

[38] F. Ajzenberg and T. Lauritsen, Revs. Modern Phys. **27**, 77 (1955).

TABLE I. Differential cross sections for scattering of 18-Mev alpha particles from neon and argon.

Neon (18.02 Mev)						Argon (17.98 Mev)					
	$Q=0$			$Q=-1.63$ Mev			$Q=0$			$Q=-1.46$ Mev	
ϕ (c.m.)	$\sigma_0(\phi)$[a] (mb/sterad)	Error[b] (%)	ϕ (c.m.)	$\sigma_1(\phi)$[a] (mb/sterad)	Error[b] (%)	ϕ (c.m.)	$\sigma_0(\phi)$[a] (mb/sterad)	Error[b] (%)	ϕ (c.m.)	$\sigma_1(\phi)$[a] (mb/sterad)	Error[b] (%)
12.3	14 600	4.2	12.5	112	11	11.4	94 300	3.2	11.5	956	12
14.5	8110	5.4	14.8	67.0	9.2	13.3	67 400	5.0	13.4	378	17
18.3	2210	4.4	18.6	66.1	7.5	16.9	20 000	5.6	22.5	36.2	32
23.6	333	3.7	24.2	48.6	7.1	21.5	6430	3.8	28.0	11.9	16
24.3	284	4.0	30.6	11.2	6.9	22.4	5120	3.8	29.8	4.55	12
30.2	167	5.9	32.8	7.90	8.9	27.8	1410	4.6	35.3	4.55	9.4
32.5	167	5.3	36.5	15.4	6.8	29.7	1190	4.5	40.7	5.53	9.6
36.1	97.8	5.7	38.7	22.7	7.3	33.3	539	4.4	46.1	2.56	13
38.3	44.4	6.2	45.3	25.1	3.1	35.1	272	6.4	49.7	1.99	16
44.2	9.37	5.6	50.4	8.99	7.3	40.5	101	5.5	51.5	1.57	18
44.8	10.7	4.7	54.0	3.52	7.1	45.9	104	5.7	55.0	2.56	12
49.9	23.6	5.8	56.2	2.93	7.3	49.4	59.1	5.9	56.8	1.95	12
53.5	32.0	5.9	59.7	5.69	7.1	51.6	40.5	6.1	60.3	1.26	10
55.6	28.8	5.6	61.8	8.44	6.3	54.8	22.7	5.7	62.1	1.23	19
59.2	14.5	6.2	65.4	10.7	4.1	56.6	15.6	5.9	65.6	0.297	15
61.2	9.53	5.7	67.5	8.78	3.6	60.1	10.4	6.6	67.4	0.228	17
64.7	0.68	7.7	70.9	10.5	3.9	61.9	12.1	6.0	70.9	0.288	13
66.8	1.28	7.8	73.0	8.20	6.3	65.4	9.83	5.5	72.6	0.744	10
70.3	4.29	5.8	76.4	6.13	7.4	67.2	7.91	6.0	76.1	0.710	8.9
72.4	8.17	6.1	78.5	6.31	7.5	70.6	4.52	6.1	77.8	0.616	11
75.8	9.88	6.0	81.8	5.80	7.9	72.4	2.15	5.9	81.2	0.639	10
77.8	11.1	5.4	83.8	6.74	5.6	75.8	1.62	6.0	83.0	0.369	11
81.1	8.82	6.5	87.1	7.27	5.2	77.6	2.09	5.9	85.9	0.176	16
83.2	6.16	5.3	89.1	8.40	5.6	81.0	2.97	6.2	88.1	0.162	15
86.4	2.59	5.9	92.4	6.96	5.4	82.7	3.27	5.9	91.4	0.164	15
88.4	1.25	8.5	94.3	7.93	6.0	86.1	2.25	6.5	93.1	0.226	10
91.7	1.50	8.3	97.5	4.56	5.9	87.8	1.92	5.8	96.4	0.263	9.8
93.6	3.65	5.9	99.4	4.95	7.2	91.1	0.988	6.3	98.1	0.304	8.9
96.8	3.98	6.0	102.5	3.19	7.2	92.8	0.394	7.7	101.4	0.231	11
101.8	4.00	6.2	104.4	2.48	7.2	96.1	0.119	14	103.1	0.180	12
103.7	3.18	6.0	107.4	2.51	6.3	97.8	0.215	11	106.3	0.154	14
106.8	2.52	5.9	109.3	3.18	5.5	101.1	0.466	7.4	108.0	0.156	14
108.6	1.73	6.1	112.3	4.98	5.6	102.8	0.718	6.0	111.2	0.169	13
111.7	3.93	6.0	114.1	5.72	4.9	106.0	0.871	5.8	112.8	0.201	11
113.4	4.03	5.5	117.1	6.25	5.5	107.7	0.948	5.8	116.0	0.157	13
116.4	5.84	5.4	118.8	5.41	5.9	110.9	0.799	5.9	117.7	0.163	12
118.2	4.90	5.9	121.7	4.27	6.7	112.6	0.543	6.9	120.8	0.150	13
121.1	4.37	6.2	123.5	3.09	6.2	115.8	0.308	9.0	122.5	0.123	14
122.8	1.92	5.7	126.3	2.44	5.2	117.4	0.152	13	125.6	0.122	14
125.7	0.72	9.2	128.0	1.74	5.9	120.6	0.107	15	127.2	0.145	13
127.4	0.58	9.7	130.8	1.95	7.1	122.2	0.122	14	131.9	0.158	12
130.2	3.15	6.7	132.5	2.75	7.1	125.4	0.203	11	135.0	0.135	13
131.9	5.03	5.8	135.3	3.44	7.1	127.0	0.224	10	136.6	0.092	15
134.7	8.61	5.6	136.9	4.72	6.6	130.1	0.234	9.8	139.7	0.078	16
136.3	9.39	5.9	139.6	4.54	6.8	131.7	0.180	11	141.3	0.075	16
139.1	12.5	5.6	141.2	4.19	7.2	134.8	0.153	12	144.3	0.070	16
140.7	7.50	5.7	143.9	4.04	6.8	136.4	0.104	14	145.9	0.081	15
143.4	6.56	6.2	145.4	4.87	5.8	139.5	0.038	23	148.9	0.104	13
145.0	2.88	5.6	148.1	3.74	5.5	141.0	0.034	24	150.4	0.179	9.7
147.7	1.09	9.5	149.6	4.05	4.1	144.1	0.016	33	153.4	0.174	9.1
149.2	1.14	7.3	152.2	5.13	5.8	145.6	0.030	25	155.0	0.185	8.8
151.9	3.00	5.9	153.8	5.41	6.3	148.7	0.049	18	157.9	0.176	8.4
153.3	6.09	5.7	156.3	7.61	6.4	150.2	0.082	14	159.5	0.131	9.5
156.0	9.19	5.5	157.8	7.98	6.3	153.2	0.157	9.6	162.4	0.089	11
157.5	8.36	5.8	160.1	10.9	7.0	154.8	0.189	8.7	164.0	0.095	11
160.1	11.1	6.6	161.9	10.8	4.9	157.8	0.251	7.0	166.9	0.087	9.3
161.6	9.31	5.0	164.4	14.1	3.9	159.3	0.247	6.9			
164.1	4.92	6.3	165.9	10.8	4.4	162.3	0.216	6.8			
165.6	3.34	6.2	168.4	10.4	4.0	163.9	0.130	9.3			
168.1	2.02	6.0	169.8	11.5	5.2	166.9	0.064	11			
169.6	3.75	6.3	172.3	10.7	4.8	168.4	0.052	11			
172.1	8.19	5.3				171.4	0.114	6.5			

[a] Cross section in the center-of-mass system.
[b] Standard deviation for number of tracks counted.

$=\pi/\{2k\Delta[\sin(\phi/2)]\}$ and the average value of the interaction radius was found to be $R=6.36\times10^{-13}$ cm.

In Fig. 8 the square of the second-order spherical Bessel function, $[j_2(qR)]^2$, is fitted to σ_1. The best agreement with the positions of the first two minima and the first maximum is obtained for $R=6.71\times10^{-13}$ cm. The minima show fair agreement with the first few zeros of $(j_2)^2$ but fail to agree for $\phi>110°$.

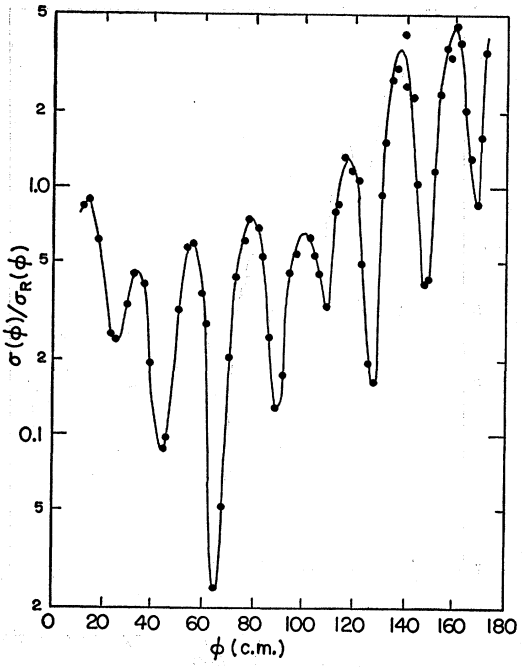

FIG. 7. Ratio of observed elastic scattering cross section to Rutherford cross section for Ne. $E_\alpha = 18.0$ Mev.

The cross sections for the shorter-range alpha-particle groups, σ_2, σ_3, σ_4, and σ_5 are plotted in Fig. 9. They are, respectively, the differential cross sections for the excitation of the 4.25-, 4.97-, 5.81(5.63)-, 7.18-, and 7.22-Mev levels of Ne^{20}, the latter two unresolved in σ_5. The zeros of $(j_2)^2$ and $(j_4)^2$ ($R = 6.71 \times 10^{-13}$ cm) for each case are also indicated. There is no clear agreement with any cross section nor is there any agreement for $(j_3)^2$, the zeros of which fall midway between those of $(j_2)^2$ and $(j_4)^2$.

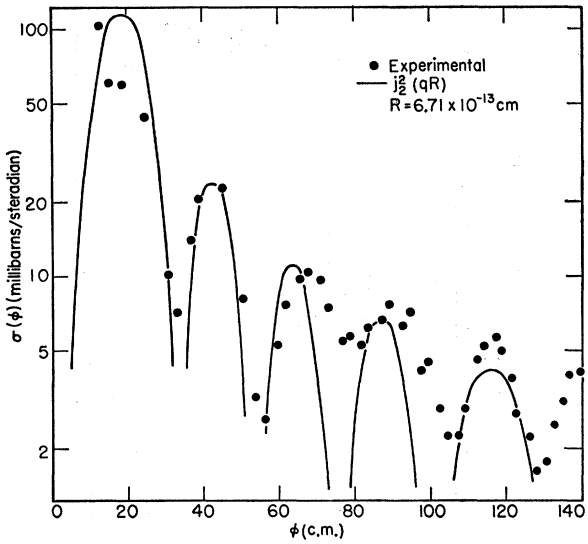

FIG. 8. Comparison of the inelastic scattering from the first excited state of Ne^{20} with direct-interaction theories.

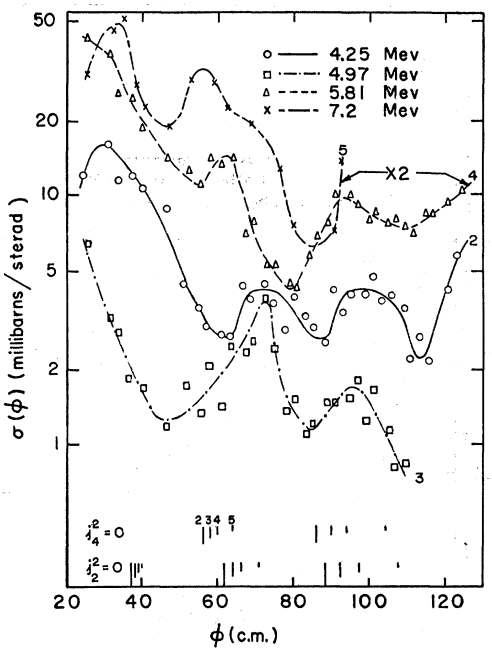

FIG. 9. Inelastic scattering cross sections of Ne^{20}, $Q < -4$ Mev.

As in the case of neon, the maxima of $\sigma_0(\phi)$ for argon (Fig. 10) are approximately equidistant in ϕ, not $\sin(\phi/2)$. The diffraction analysis yields $R = 6.95 \times 10^{-13}$ cm. The ratio σ_0/σ_R is plotted in Fig. 11. The differential cross section for inelastic scattering is shown in Fig. 12, together with $[j_2(qR)]^2$, $R = 6.60 \times 10^{-13}$ cm.

In Fig. 13, the values of $\sigma_0(\phi)/\sigma_R(\phi)$ for xenon are plotted. It is difficult to judge if, over the limited range investigated, the deviations from Rutherford scattering are real. The standard deviations shown include effects of the uncertainty in the angular setting and of the reliability of the number of tracks counted. The standard deviation arising from the uncertainty in the energy (ΔE) is indicated by the two dashed lines. The weighted mean value of $\sigma_0(\phi)/\sigma_R(\phi)$ is 1.054 ± 0.033. The probability of the chance occurrence of this deviation is about $\frac{1}{9}$.

Discussion

The pronounced structure in the elastic scattering cross sections (neon and argon) and the lack of symmetry about 90° in any of the inelastic scattering cross sections appear to preclude compound-nucleus formation as a principal mechanism for the reactions. In the elastic cases, the angular distributions are typical of those predicted by the optical model,[20,21] although the calculations required for detailed comparison have not yet been made. The well defined minima indicate that λ, the mean free path for absorption of alpha particles, must be quite small. The pronounced oscillations contrast with those generally found in the case of (p,p)

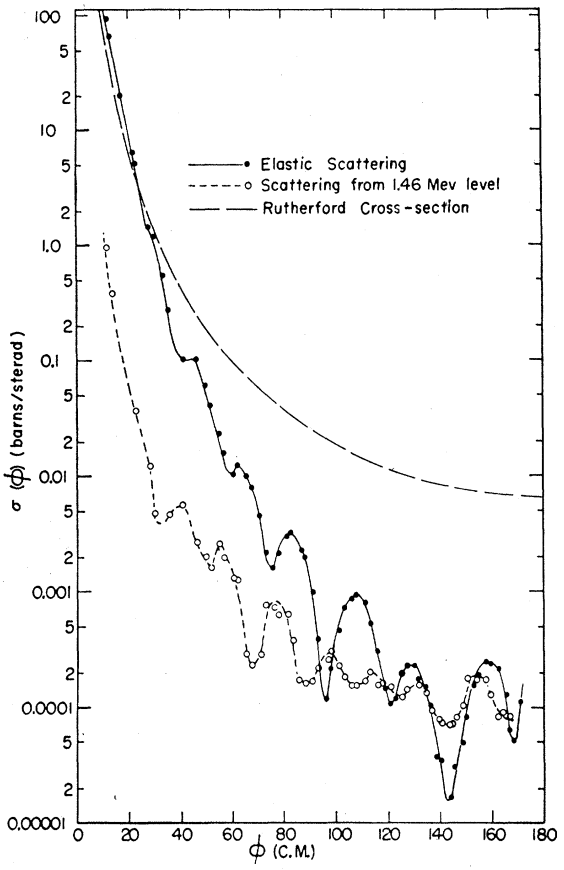

FIG. 10. Scattering cross sections for argon. $E_\alpha = 18.0$ Mev.

and (p,p') scattering (e.g., Dayton and Schrank,[39] Freemantle *et al.*[40]), which imply a larger value of λ for protons. This is borne out by typical values for λ derived from the experimental data by means of the optical model: 10-Mev protons, 5×10^{-13} cm [18]; 20-Mev protons, 3×10^{-13} cm [21]; 22-Mev alpha particles, 1.5×10^{-13} cm [21]; and 20–40 Mev alpha particles, $\sim1\times10^{-13}$ cm.[18] The smeared-out structure of the proton angular distributions can be understood as due either to a large proportion of compound-nucleus formation or to a spread in the depth at which the direct interaction takes place or both. Contrarywise, the alpha-particle angular distributions are more oscillatory.

The agreement of the second-order spherical Bessel functions with the first excited state distributions for both Ne^{20} and A^{40} is consistent with the spins and parities of the levels involved and the selection rules of Austern *et al.*[22] and of Hayakawa and Yoshida.[23] The ground states are both 0^+ and the first excited states are both 2^+. The selection rule of Austern *et al.* for a spinless particle becomes $l_{\min} \geqslant \Delta J$, $l_{\min}$ being odd or even depending on whether the nucleus changes parity

[39] I. E. Dayton and G. Schrank, Phys. Rev. **101**, 1358 (1956).
[40] Freemantle, Prowse, Hossain, and Rotblat, Phys. Rev. **96**, 1270 (1954).

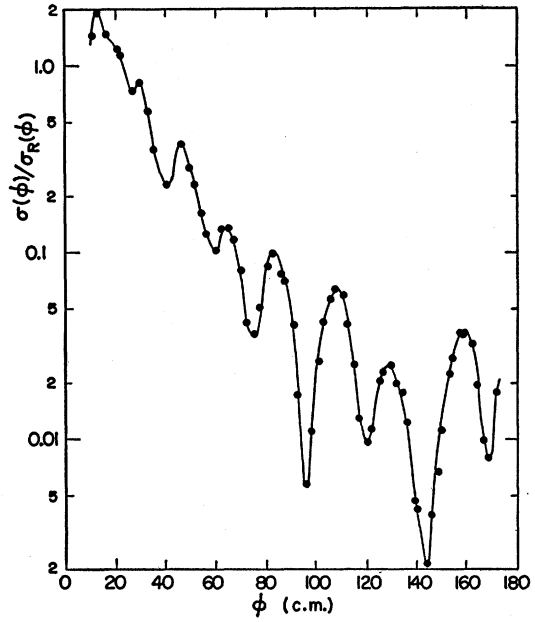

FIG. 11. Ratio of observed elastic scattering cross section to Rutherford cross section for argon. $E_\alpha = 18.0$ Mev.

or not. The agreement is good with respect to the location of the first few minima, but is extremely poor in the forward direction. The theories predict a small cross section at 0° (for the particular reactions studied), but large forward peaks are observed. As mentioned in the introduction, in these calculations the incident and scattered wave functions are approximated by plane waves. The calculations of Levinson and Banerjee[26] for the case of $C^{12}(p,p')$, $Q=-4.43$ Mev, which include the effects of potential distortion, reproduce the forward

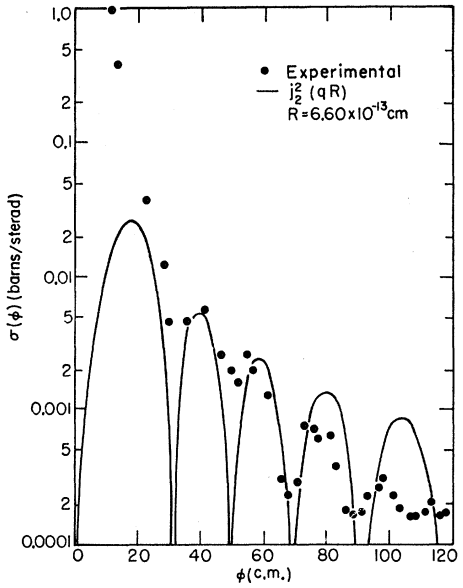

FIG. 12. Comparison of the inelastic scattering from the first excited state of A^{40} with direct-interaction theories.

peaking observed in that reaction for which the Austern-Butler-McManus theory predicts low forward intensity.

The failure to obtain a similar agreement between the squares of a spherical Bessel function and the differential cross sections for inelastic scattering from the higher excited states of neon (Fig. 9) is consistent with the expectation that reactions leading to the lowest excitation have a greater probability of proceeding through a direct interaction than those involving higher excitation.[24] σ_1, however, is of the same order of magnitude as σ_2, σ_3, σ_4, and σ_5, so that the latter probably are not due solely to compound-nucleus formation.

No information exists in the literature regarding the spins or parities of the 4.25-, 4.97-, or 5.81(5.63)-Mev

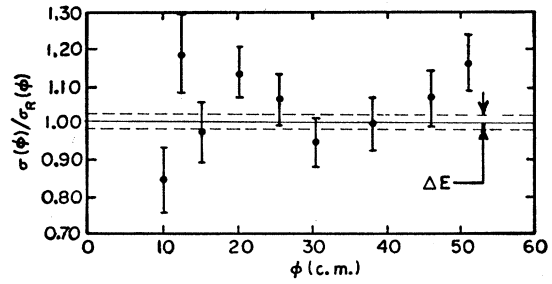

FIG. 13. Ratio of observed elastic scattering cross section to Rutherford cross section for Xe. $E_\alpha = 18.3$ Mev.

levels. A 6.74-Mev level (not observed here) has spin and parity 0^+; the 7.18-Mev level has 3^- and the 7.22-Mev level has 0^+.[38] It is possible that the 6.74-Mev (0^+) state is due to a collective "breathing" surface vibration, carrying zero angular momentum. If this is so, alpha particles would not seem to be effective in exciting such states. On the other hand, if the level were an individual-particle state, one would expect a small probability for a $0^+ - 0^+$ transition because of the small overlap of the orthogonal wave functions describing the two states. Since the 7.22-Mev level is also 0^+, it is reasonable to conclude that σ_5 represents primarily the distribution of alpha particles exciting the 3^- level at 7.18 Mev. It is not possible, however, to obtain a good fit with $[j_3(qR)]^2$ for any value of R.

TABLE II. Alpha-nucleus interaction radii.

$R_0 = \pi/\{2k\Delta[\sin(\phi/2)]\}$ from elastic scattering, R_1 from inelastic scattering,

$R_2 = 1.50A^{\frac{1}{3}} + 2.00$, $R_3 = 1.27A^{\frac{1}{3}} + 1.60$.

All values in units of 10^{-13} cm.

Nucleus	R_0	R_1	R_2	R_3
Ne	6.36	6.71	6.07	5.04
Al	6.41	...	6.50	5.41
A	6.95	6.60	7.13	5.94

Table II summarizes the various values of R determined in this experiment together with that of Al found by Gailar.[27] Also given are the values calculated from $R_2 = 1.50A^{\frac{1}{3}} + 2.00$ (in units of 10^{-13} cm) and finally, in the last column, the values obtained from the relation $R_3 = 1.27A^{\frac{1}{3}} + 1.60$ which gives the trend of the values found by Igo *et al.*[9] at 40 Mev.

It is apparent from Table II that the interaction radii calculated in this simple manner are energy-dependent. Our radii are consistently larger than those found by Igo *et al.*, agreeing more closely with R_2 than with R_3. An actual optical-model analysis would be necessary for a meaningful comparison between the results at 40 Mev and those at 18 Mev.

ACKNOWLEDGMENTS

Our appreciation is extended to Mrs. Lillian Henriksen and Mr. M. Livingston for their conscientious and meticulous scanning of the nuclear track plates. Dr. O. H. Gailar, H. H. Brewer, W. E. Jordan, and J. Moore aided in the construction of the scattering chamber. Mr. F. Hobaugh helped with the cyclotron bombardments. One of us (L. S.) wishes to thank Dr. C. A. Levinson and Dr. M. K. Banerjee for informative discussions and for permission to quote results before publication.

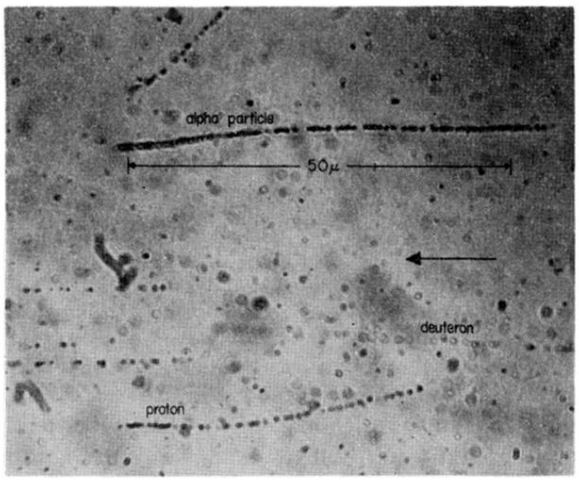

FIG. 3. Differentially developed tracks in $E1$ emulsion.